International Journal of Latest Trends in Engineering and Technology
Vol.(10)Issue(2), pp.365-380
DOI: http://dx.doi.org/10.21172/1.102.59
e-ISSN:2278-621X

VOLTAGE CONTROL OF A DC LINK IN ROTOR SIDE CONVERTER FOR A WT BASED DFIG

M.Ramesh[1], T.R.Jyothsna[2]

Abstract- The existence of voltage ripples across the DC link of the rotor side converter of a DFIG is inherent due to uncertainty in wind energy as well as the variation of rotor angular velocity. This can deteriorate the performance of the back-to-back converter connected on the rotor side of the DFIG. Hence, the main objective of this paper is to design a feedback linearization technique to eliminate the dc-link voltage ripple as well as obtain unity power factor. In this paper, the dynamic modeling of DFIG along with the rotor side converter is performed. The feedback linearization technique controls the internal dynamics of the rotor side converter by considering the rotor q-axis current and DC link voltage. The MATLAB simulation results depict the efficacy of the voltage control method, through the variations of rotor side filter, DC link capacitance and uncertainties in the DC link voltage.
Keywords – Rotor side converter, DC link voltage, Feedback linearization, Voltage control

1. INTRODUCTION

Wind power generations have been growing rapidly all over the world and have become one of the most promising renewable generation technologies. Among the different types of the wind energy conversion system (WECS), doubly fed induction generator (DFIG)[1] based wind energy conversion systems have gained the increasing proportion due to the tremendous benefits, which include the variable speed constant frequency operation, four-quadrant active and reactive power capabilities, smaller converters rating (around 30% of the generator rating), lower cost and power losses, compared with any fixed-speed induction generators and synchronous generators[1]. Normally, DFIG-based WECSs are supplied by the rotor with back to back converter. Back to back converter consists of rotor side converter and grid side converter [2], [3]. The two level rotor side converter feeds rotor of DFIG. The control of rotor side converter along with DC link is emphasized in this paper.

An averaged small-signal technique has been applied by near-optimum feed-forward compensator in [4]. Constant DC link voltage as well as unity power factor under different load conditions has been obtained for PWM based AC to DC converters in [5]-[11].A substantial reduction of DC capacitance is obtained by using a state feedback based control strategy in [7].A current-control-based control strategy utilized a proportional plus integral controller to generate a command signal for the input line current amplitude in [8]. The input output feedback linearization method has been applied in [9] - [11].

This paper proposed the application of feedback linearization technique from differential geometric theory to the implementation of constant DC link voltage [12][13] and unity power factor control of rotor side converter in doubly fed induction generator. In this study detailed analysis of applying feedback linearization technique to the control [14]-[16] of rotor side converter is performed based on the dynamic modeling of converter. Here, the control strategy is chosen as voltage control to linearize the rotor side converter with output variables as rotor side q-axis current and DC link voltage [6], [7], and [16]. Later internal dynamics [17]–[19] of the rotor side converter is applied through the voltage control. Finally effectiveness of the proposed voltage control strategy is presented through the simulation results.

This paper will be organized as follows. First, Section II describes the dynamic modeling of the DFIG and rotor side converter. Then, the control schemes for the RSC, using feedback linearization technique and its detailed analysis of input output linearization is presented and Implementation of internal dynamics of the rotor side converter through voltage control is given in section III. Simulation results are showcased in Section IV. Finally, section V summarizes the conclusions.

2. MODELING OF DFIG AND RSC

Steady state and dynamic modeling of DFIG

The schematic diagram of DFIG based wind conversion system with [1] rotor side converter is shown in Fig.1. The wind system consists of wind turbine, DFIG, rotor side converter, DC link and grid side converter. DFIG primarily consists of stator and rotor three phase windings [2] which are energized separately and both windings can supply energy bi-directionally. The rotor windings can be connected in delta or star. Stator is energized by the grid at constant balanced three phase supply and the rotor is energized by back to back converter at constant balanced three phase supply but independently from the stator. Steady state voltage equations of stator and rotor are presented in following equations.

[1] Department of Electrical Engineering Andhra University College of Engineering (A), Visakhapatnam, A.P, India
[2] Department of Electrical Engineering, Andhra University College of Engineering (A), Visakhapatnam, A.P, India

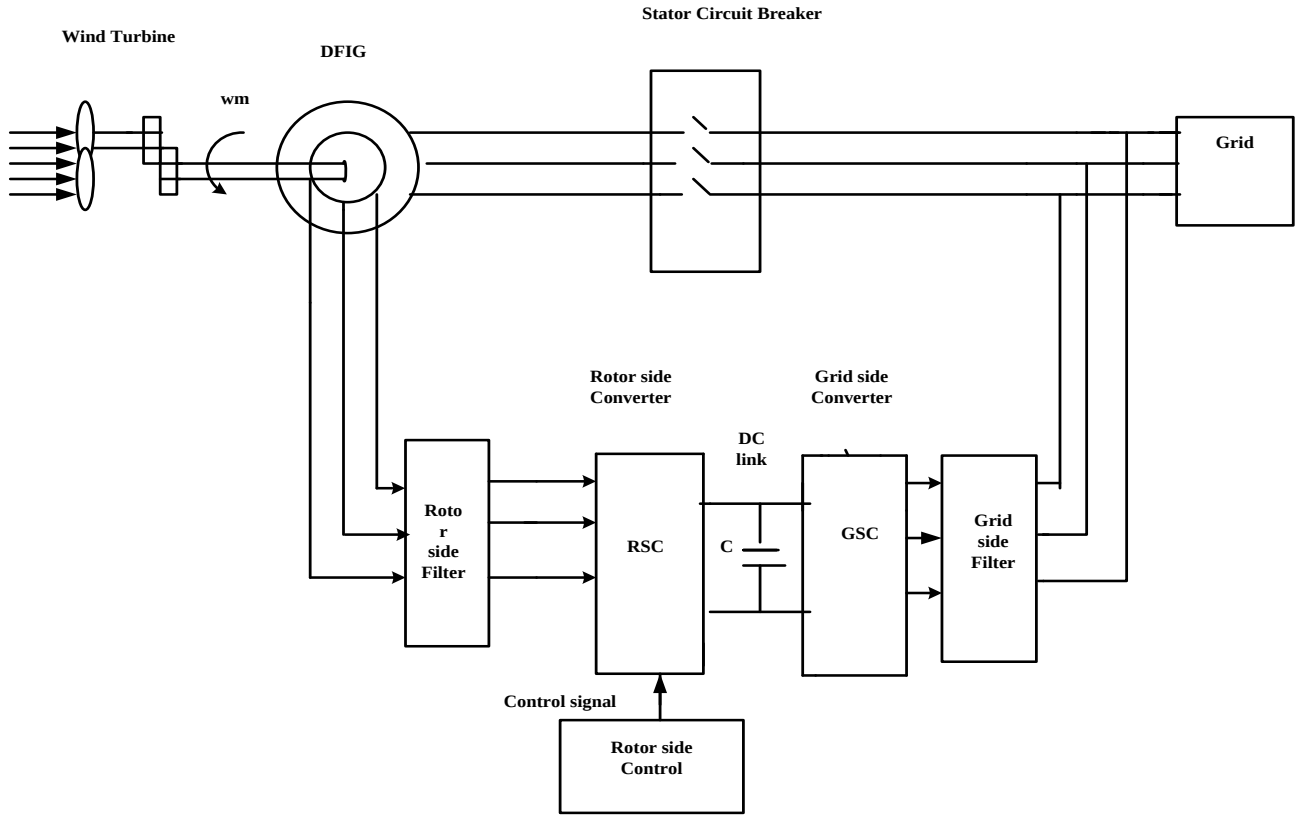

Fig.1 Schematic Diagram of DFIG Based Wind System

Stator voltage equations:

$$V_{as} = R_s i_{as} + j\omega_s \psi_{as} \quad (1)$$

$$V_{bs} = R_s i_{bs} + j\omega_s \psi_{bs} \quad (2)$$

$$V_{cs} = R_s i_{cs} + j\omega_s \psi_{cs} \quad (3)$$

Rotor voltage equations:

$$V_{ar} = R_r i_{ar} + j\omega_r \psi_{ar} \quad (4)$$

$$V_{br} = R_r i_{br} + j\omega_r \psi_{br} \quad (5)$$

$$V_{cr} = R_r i_{cr} + j\omega_r \psi_{cr} \quad (6)$$

Stator and Rotor *d-q* equations:

$$V_{ds} = R_s i_{ds} + \frac{d\psi_{ds}}{dt} - j\omega_s \psi_{qs} \quad (7)$$

$$V_{qs} = R_s i_{qs} + \frac{d\psi_{qs}}{dt} + j\omega_s \psi_{ds} \quad (8)$$

$$V_{dr} = R_r i_{dr} + \frac{d\psi_{dr}}{dt} + j(\omega_s - \omega_r)\psi_{qr} \quad (9)$$

$$V_{qr} = R_r i_{qr} + \frac{d\psi_{qr}}{dt} - j(\omega_s - \omega_r)\psi_{dr} \quad (10)$$

2.1 Mathematical modeling of RSC

The power circuit of RSC topology shown in Fig.2 is composed of six controlled switches and rotor input filter. AC side inputs are ideal three-phase symmetrical rotor voltages, which are filtered by resistance and inductance, then connected to three phase rotor side converter consist of six IGBTs and diodes in anti-parallel[1], [3],[5]. The output is composed of DC link capacitance and inverter parameters.

The model of RSC is carried out under the following assumptions.

The power converter switches are ideal devices.

All the parameters are Linear time invariant

The three phase voltages are balanced.

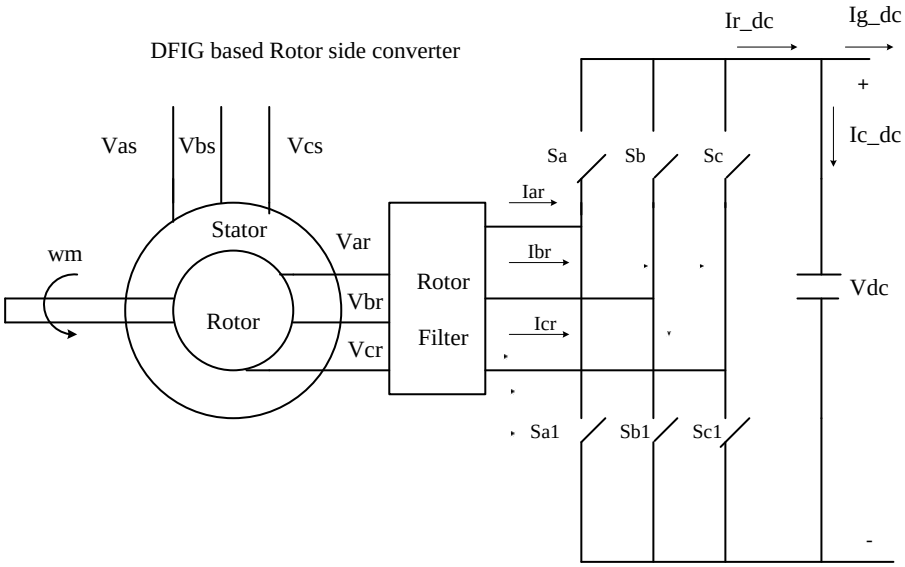

Fig.2 Schematic diagram of rotor side converter

2.2 Rotor side Converter equations:

$$V_{dr} = R_f\, i_{dr} + L_{dc}\left(\frac{di_{dr}}{dt}\right) - \omega_{rL_{dc}} i_{qr} + V_{do} \quad (11)$$

$$V_{qr} = R_f\, i_{qr} + L_{dc}\left(\frac{di_{qr}}{dt}\right) + \omega_{rL_{dc}} i_{dr} + V_{qo} \quad (12)$$

$$C\frac{dV_{dc}}{dt} = (u_d i_{dr} + u_q i_{qr}) - (i_{g\_dc}) \quad (13)$$

$$V_{do} = u_d V_{dc}\ V_{qo} = u_q V_{dc} \quad (14)$$

2.3 Controller state equations:

$$\frac{di_{dr}}{dt} = -\left(\frac{R_f}{L_{dc}}\right) i_{dr} + \omega_r i_{qr} + \frac{V_m}{L_{dc}} - \frac{(u_d V_{dc})}{L_{dc}} \tag{15}$$

$$\frac{di_{qr}}{dt} = -\left(\frac{R_f}{L_{dc}}\right) i_{qr} - \omega_r i_{dr} - \frac{(u_q V_{dc})}{L_{dc}} \tag{16}$$

$$\frac{dV_{dc}}{dt} = \frac{1}{C}(u_d i_{dr} + u_q i_{qr}) - \frac{1}{C}(i_{g\_dc}) \tag{17}$$

where

V_m Maximum value of the rotor input voltage

V_{dc} DC link capacitor

R_f Resistance of the rotor side filter

L_{dc} Inductance of the rotor side filter

In the transformed state equations from (15) to (17), the space vector is defined as X = [*idr iqr Vdc*] and the control input vector u = [ud uq] is the switching functions u = [*ua ub uc*] is synchronously rotating *d-q* quantities. The aim of the model is to achieve the constant DC link voltage and unity power factor. It can be obtained by regulating the value of *q*-axis current to zero and dc link voltage traces the given dc link reference voltage *Vdc_ref* [10]. From the control perception, modeling the rotor side converter in d-q reference frame has the advantage of the reducing the time varying quantities in required state equations.

3. FEEDBACK LINEARIZATION TECHNIQUE

3.1 Steady Input output feedback Linearization

At present, the input output linearization technique is utilized as a design method to linearize the non linear system. Unlike linear approximations of the internal dynamics, in input output linearization technique exact state transformations are used to carry the process of linearization. Moreover the actual system is converted into simplest form [2][3][11]. In input output linearization technique, selecting the new auxiliary control variables which facilitate to reduce the tracing error to nullify the non-linearity [17]-[19].

The non-linear state equations (15) to (17) of the rotor side converter are rearranged in the following equation (18). Three quantities f(x), g(x) and X are arranged in matrix form and at the end they are shown as complete equation. This state vector and output vector y play an important role in finding the values of the control signals and there by switching signals for rotor side converter. According to the theory of [7] input output linearization one must choose a dummy output vector y= [y1 y2], reference vector y*= [y1* y2*] and tracing error e = [y - y*].

$$f(x) = \begin{bmatrix} -\left(\frac{R_f}{L_{dc}}\right) i_{dr} + \omega_r i_{qr} + \frac{V_m}{L_{dc}} \\ -\left(\frac{R_f}{L_{dc}}\right) i_{qr} - \omega_r i_{dr} \\ -\frac{1}{C}(i_{g\_dc}) \end{bmatrix} \quad g(x) = \begin{bmatrix} -\frac{(V_{dc})}{L_{dc}} & 0 \\ 0 & \frac{(V_{dc})}{L_{dc}} \\ \frac{1}{C}(i_{dr}) & \frac{1}{C}(i_{qr}) \end{bmatrix}$$

$$\dot{X} = \begin{bmatrix} -\left(\frac{R_f}{L_{dc}}\right) i_{dr} + \omega_r i_{qr} + \frac{V_m}{L_{dc}} \\ -\left(\frac{R_f}{L_{dc}}\right) i_{qr} - \omega_r i_{dr} \\ -\frac{1}{C}(i_{g\_dc}) \end{bmatrix} + \begin{bmatrix} -\frac{(V_{dc})}{L_{dc}} & 0 \\ 0 & \frac{(V_{dc})}{L_{dc}} \\ \frac{1}{C}(i_{dr}) & \frac{1}{C}(i_{qr}) \end{bmatrix} \begin{bmatrix} u_d \\ u_q \end{bmatrix}$$

$$\dot{X} = f(x) + g(x)u \tag{18}$$

3.2 Voltage control

Using the theoretical results described in the previous section, we present here a input output linearizing solution, denoted as voltage control [2][4][6][9] for the dc-bus voltage control of rotor side converter with unity power factor by choosing two different dummy output variables. The dummy output variables are chosen as *y* = [*iqr Vdc*] since the aim is to maintain the DC link voltage *Vdc* is equal to voltage reference *Vdc_ref* with q-axis current iqr is zero [13][16]. Then reference output vector must be *y** = [*0 Vdc_ref*] according to the procedure of input output linearization technique.

$$\begin{bmatrix} u_d \\ u_q \end{bmatrix} = \begin{bmatrix} 0 & -\frac{(V_{dc})}{L_{dc}} \\ \frac{1}{C}(i_{dr}) & \frac{1}{C}(i_{dr}) \end{bmatrix}^{-1} \left(\begin{bmatrix} \omega_r i_{qr} + \left(\frac{R_f}{L_{dc}}\right) i_{dr} \\ \frac{1}{C}(i_{g\_dc}) \end{bmatrix} + \begin{bmatrix} -K_{10} i_{qr} \\ -K_{20}\left(V_{dc} - V_{dc\_ref}\right) \end{bmatrix} \right) \tag{19}$$

Now the internal dynamics are

$$\frac{di_{dr}}{dt} = -\left(\frac{R_f}{L_{dc}}\right) i_{dr} + \frac{V_m}{L_{dc}} - \frac{(V_{dc})}{L_{dc}} \left(\frac{ig\_dc}{idr}\right) + \left(\frac{K_2}{i_{dr}}\right)(CV_{dc}(V_{dc} - V_{dc\_ref}) - \left(\left(\frac{R_f}{L_{dc}} - K_1\right)\left(\frac{i^2_{qr}}{i_{dr}}\right)\right) \tag{20}$$

Tracing error e to zero where iqr tends to zero [4], [12] and DC link voltage Vdc is approaches to DC link voltage reference. After obtaining the zero dynamics of the system, two equilibrium points are:

$$i_{dr\_ref} = \frac{1}{2}\left[\frac{V_m}{R_f} \pm \sqrt{\left(\frac{V_m}{R_f}\right)^2 - \left(\frac{4V_{dc\_ref}\, i_{g\_dc}}{R_f}\right)}\right] \tag{21}$$

Effective equilibrium point is chosen as [4]

$$i_{dr\_ref} = \frac{1}{2}\left[\frac{V_m}{R_f} - \sqrt{\left(\frac{V_m}{R_f}\right)^2 - \left(\frac{4V_{dc\_ref}\, i_{g\_dc}}{R_f}\right)}\right] \tag{22}$$

3.3 Application of voltage control on RSC

The controlling circuit of rotor side converter [3] with input output linear voltage control is presented in Fig.3. The Voltage control diagram of RSC using Input output linearization is shown in Fig.3. Rotor abc voltages and phase angles are considered from phase voltages of DFIG Rotor.

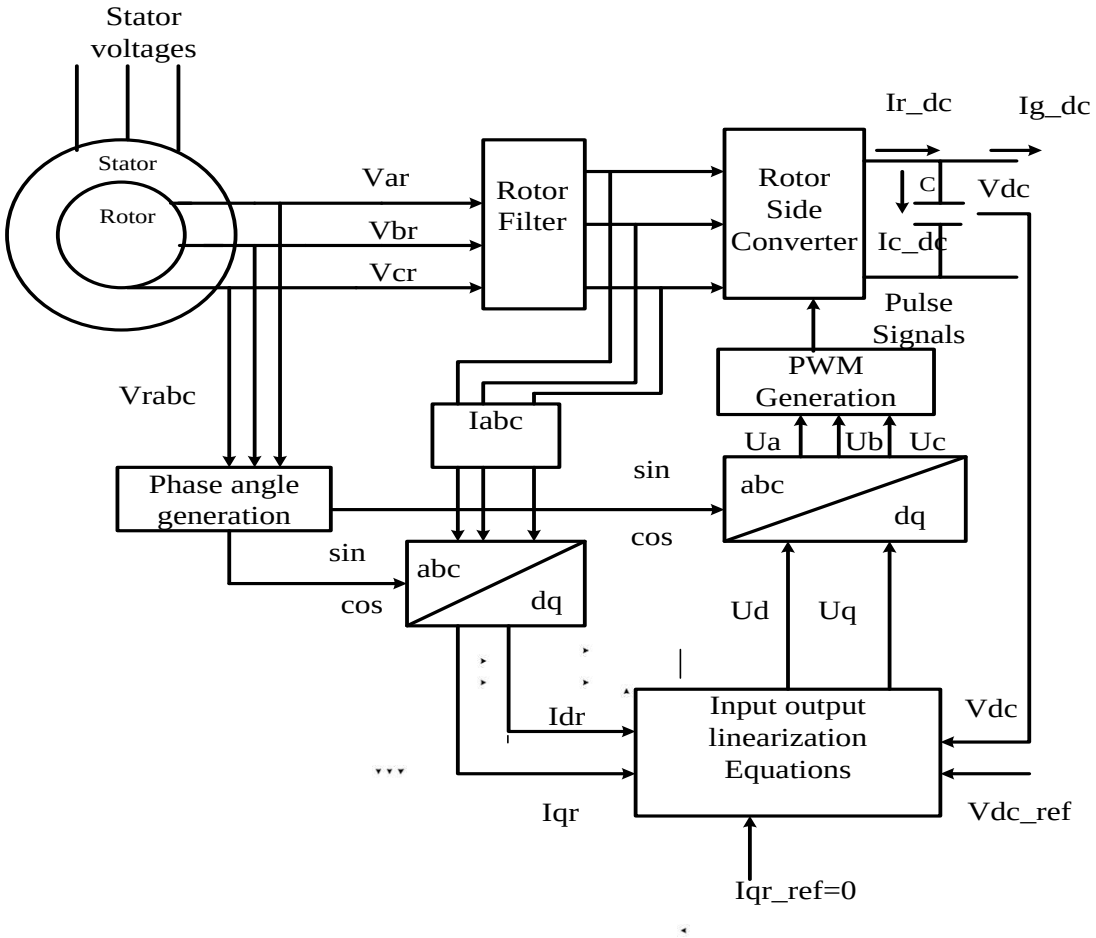

Fig.3 Input Output Linearization Voltage Control of RSC

4. SIMULATION RESULTS

The specifications and circuit parameters used in the simulation are given in Table 1. Simulation results of steady state and dynamic modeling of DFIG, variation of DC link voltage of rotor side converter with and without controller and effect of parameter uncertainties on rotor direct axis current and DC link voltage are presented in following section.

4.1 Steady State and dynamic Modeling of the DFIG

Steady state response of DFIG system is shown in Fig.4 (a) to Fig.4 (f).

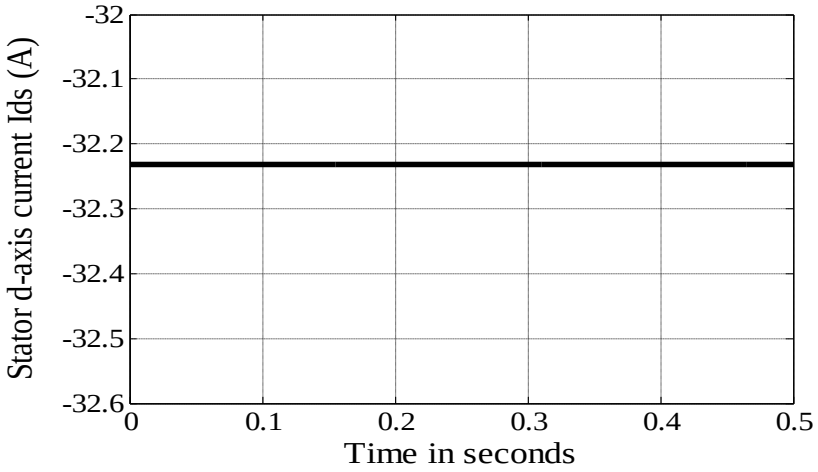

Fig .4(a) Stator *d*-axis Current i_{ds}

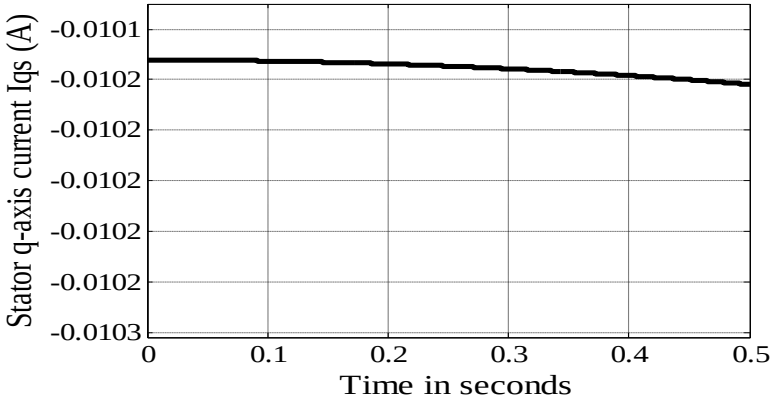

Fig.4 (b) Stator *q*-axis Current i_{qs}

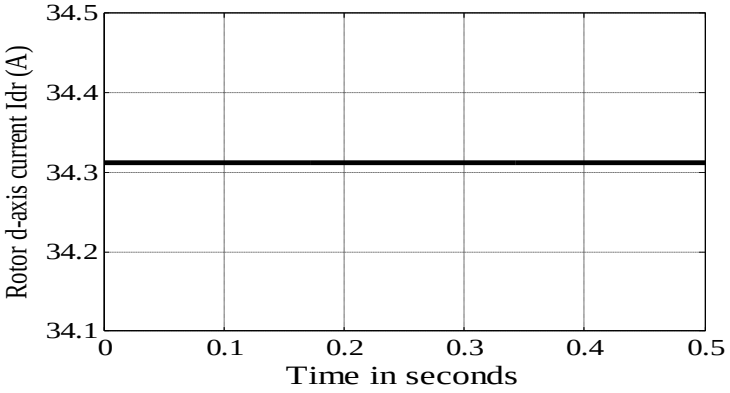

Fig .4(c) Rotor d-axis Current i_{dr}

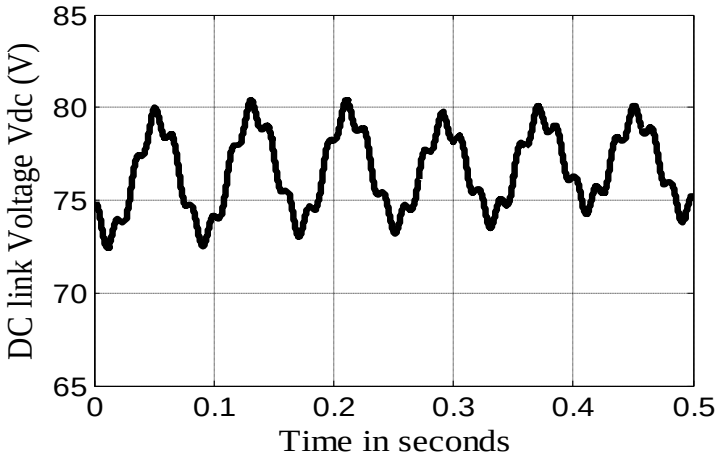

Fig.4 (d) DC Link Voltage V_{dc}

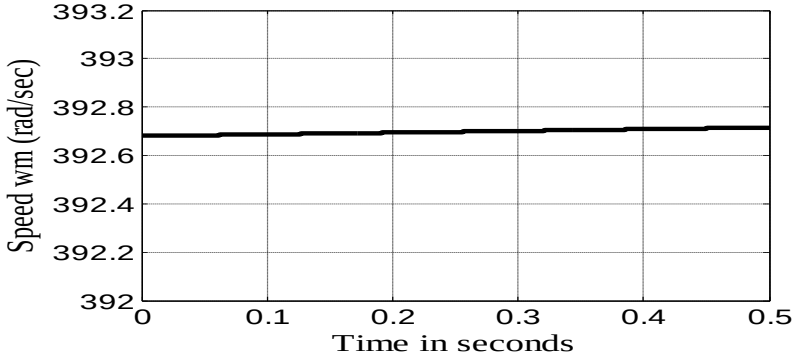

Fig.4 (e) Speed w_m of the DFIG Rotor

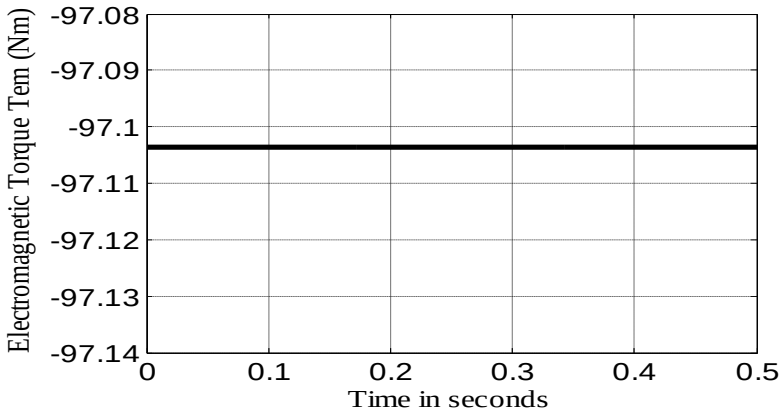

Fig.4(f)Electromagnetic Torque T_{em}

4.2 DC link voltage with and without controller

The responses of the rotor side converter with and without controllers are shown in Fig.5. In actual system there are many ripples in DC link voltage where as they are eliminated in the voltage controller. Output wave form is smoothened and maintains the constant DC link voltage throughout the system irrespective of parameter variations.

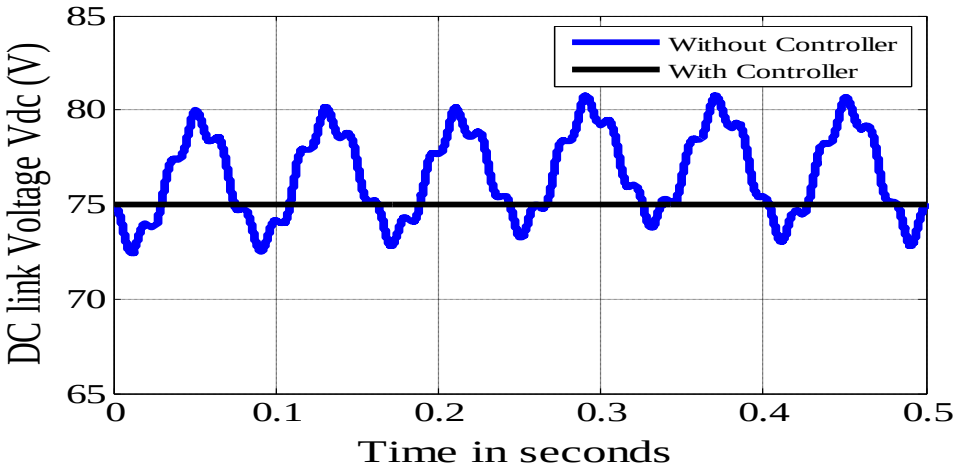

Fig.5 Variation of DC Link Voltage V_{dc} with and without Controller

4.3 Disturbance consideration and parameter uncertainties

When disturbance has occurred in the system from 0.1 to 0.12 sec and also between 0.3 to 0.32 seconds the DC link voltage is varied instantly during that period which is shown in Fig.6 (a). In case of rotor d-axis Current, the effect of disturbance is shown in Fig.6 (b) during 0.1 to 0.12 sec and 0.3 to 0.32 sec.

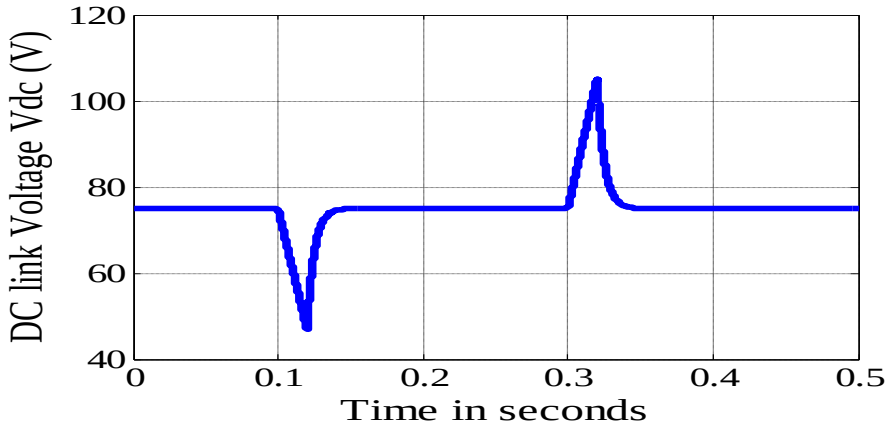

Fig.6 (a) DC link Voltage V_{dc} for perturbation in filter parameter

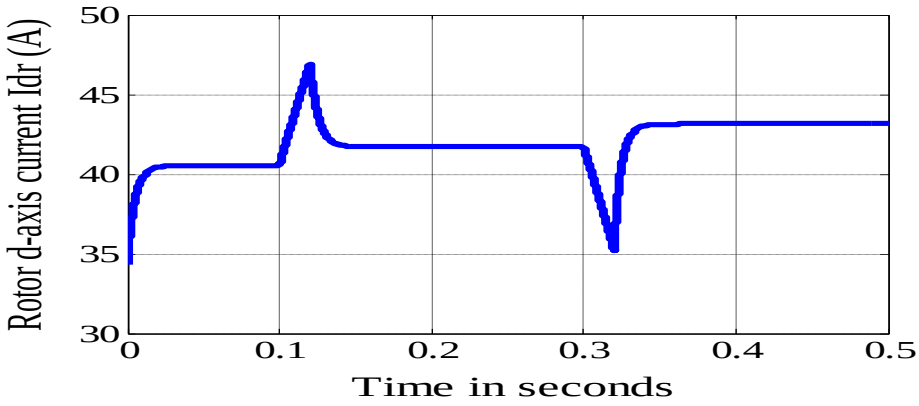

Fig.6(b) Rotor d-axis Current for pertubation in fiter parameters

The changes in wave shape of DC link and Rotor d-axis current when it is subjected to change of filter parameters from 0.1 to 0.12 sec is shown in Fig.7(a) and Fig.7(b). The variations in waveforms of DC link and rotor d-axis current when it is subjected to change in filter parameters from 0.3 to 0.32 sec is clearly shown in Figs. 8(a) and 8(b). The value of the Vdc is increaed from 75V to nearly 105V and back to original value. The effect of changes in DC link capacitance and inductance, impact on DC link Voltage Vdc and rotor d-axis current are shown in Fig. 9(a) and 9(b). With the increased values of inductance and capacitance there is no change in DC link voltage, however significant change in rotor d-axis current are clearly shown.

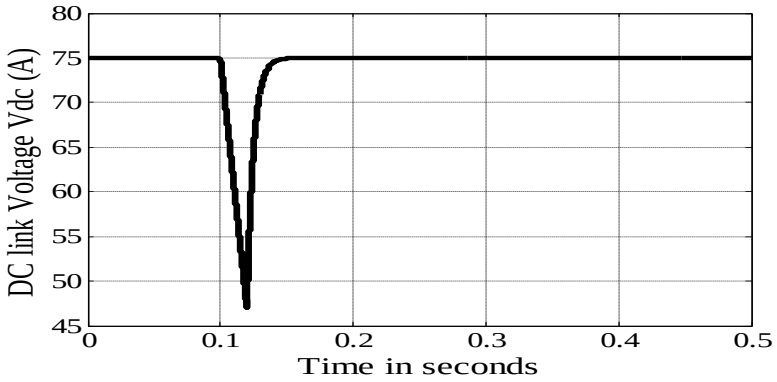

Fig .7(a) DC Link Voltage for perturbation in filter parameters

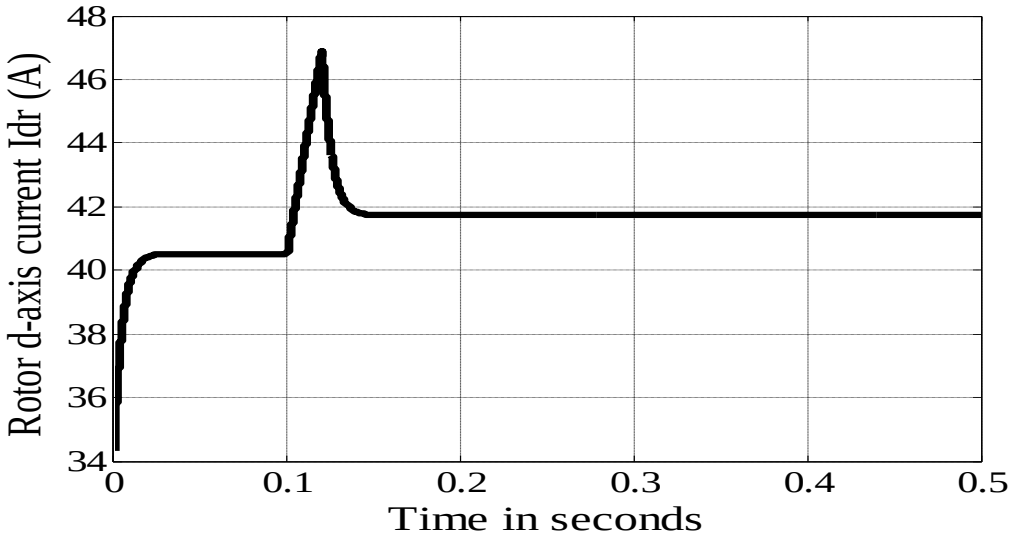

Fig.7 (b) Rotor d-axis Current i_{dr} for perturbation in filter parameters

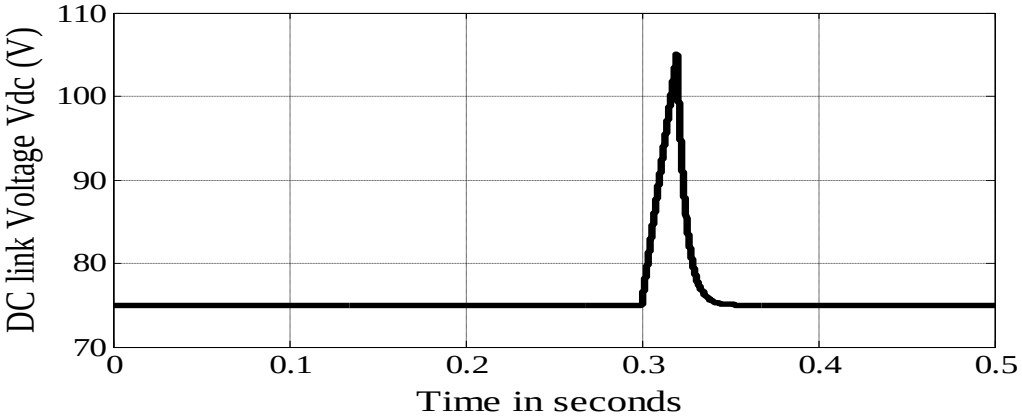

Fig .8(a) DC Link Voltage V_{dc}

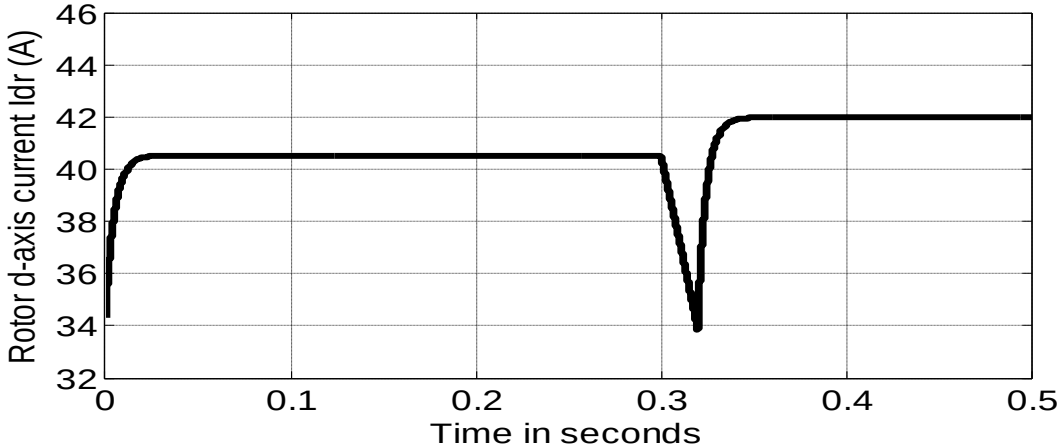

Fig.8 (b) Rotor *d*-axis Current i_{dr}

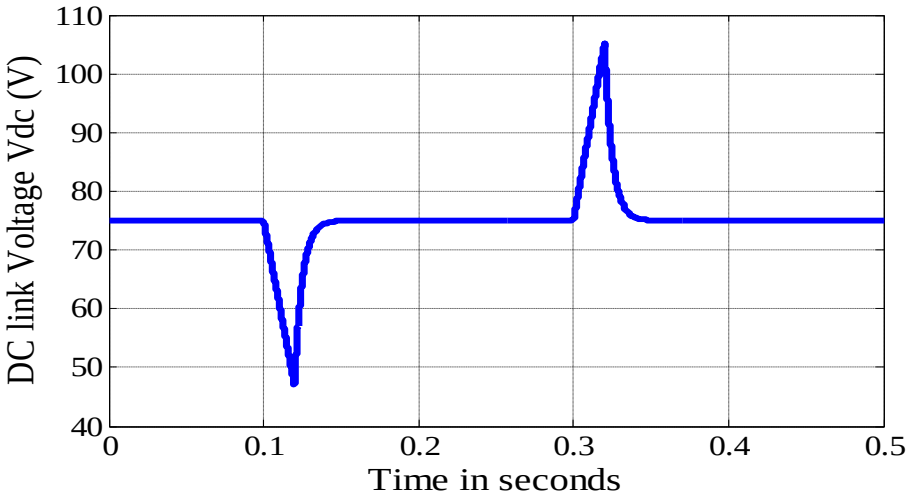

Fig.9 (a) Effect of uncertinities on DC link Voltage V_{dc}

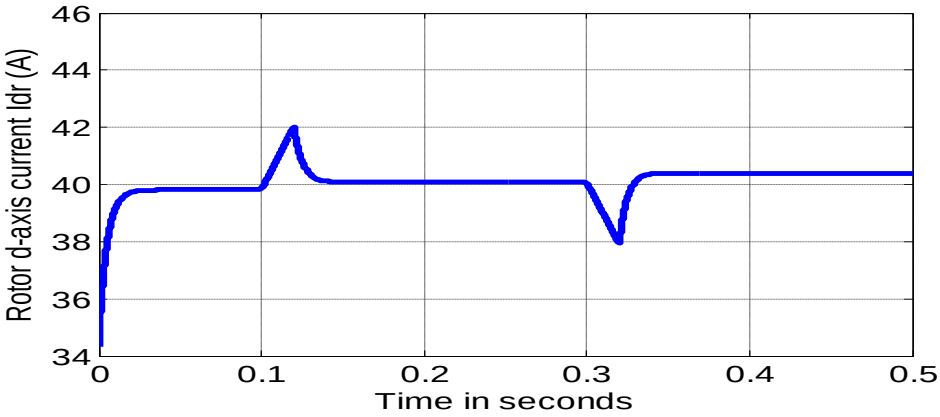

Fig.9 (b) Effect of uncertinities on Rotor *d*-axis current i_{dr}

Table.1 Specifications of the Rotor side converter DFIG

Power rating	5 kW
Source voltage	77.85V
DC link Voltage	75V
Inductor Ldc	0.08H
Resistor Rf	0.01Ω
DC Link Capacitor	2.9mF
Frequency	50 Hz
Grid side Inductor	0.08H
Grid side Resistor	0.1Ω

5. CONCLUSION

This paper proposes a voltage control of DC link voltage for rotor side converter. Constant DC link voltage and unity power factor of the system is achieved. Dynamic modeling of DFIG and mathematical modeling of the rotor side converter is presented. The performance of the rotor side converter with and without controller is clearly shown in simulation results. It is clearly found that the control strategy is robust for the variations of rotor side filter, DC link capacitance, uncertainties in the DC link voltage.

6. REFERENCES

[1] B. Corona, M. Nakano, H. Pérez, “Adaptive Watermarking Algorithm for Binary Image Watermarks”, Lecture Notes in Computer Science, Springer, pp. 207-215, 2004.

[2] A A. Reddy and B. N. Chatterji, "A new wavelet based logo-watermarking scheme," Pattern Recognition Letters, vol. 26, pp. 1019-1027, 2005.

[3] P. S. Huang, C. S. Chiang, C. P. Chang, and T. M. Tu, "Robust spatial watermarking technique for colour images via direct saturation adjustment," Vision, Image and Signal Processing, IEE Proceedings -, vol. 152, pp. 561-574, 2005.

[4] F. Gonzalez and J. Hernandez, " A tutorial on Digital Watermarking ", In IEEE annual Carnahan conference on security technology, Spain,1999.

[5] D. Kunder, "Multi-resolution Digital Watermarking Algorithms and Implications for Multimedia Signals", Ph.D. thesis, university of Toronto, Canada, 2001.

[6] J. Eggers, J. Su and B. Girod," Robustness of a Blind Image Watermarking Scheme", Proc. IEEE Int. Conf. on Image Proc., Vancouver, 2000.

[7] Barni M., Bartolini F., Piva A., Multichannel watermarking of color images, IEEE Transaction on Circuits and Systems of Video Technology 12(3) (2002) 142-156.

[8] Kundur D., Hatzinakos D., Towards robust logo watermarking using multiresolution image fusion, IEEE Transcations on Multimedia 6 (2004) 185-197.

[9] C.S. Lu, H.Y.M Liao, “Multipurpose watermarking for image authentication and protection,” IEEE Transaction on Image Processing, vol. 10, pp. 1579-1592, Oct. 2001.

[10] L. Ghouti, A. Bouridane, M.K. Ibrahim, and S. Boussakta, “Digital image watermarking using balanced multiwavelets”, IEEE Trans. Signal Process., 2006, Vol. 54, No. 4, pp. 1519-1536.

[11] P. Tay and J. Havlicek, "Image Watermarking Using Wavelets", in Proceedings of the 2002 IEEE, pp. II.258 – II.261, 2002.

[12] P. Kumswat, Ki. Attakitmongcol and A. Striaew, "A New Approach for Optimization in Image Watermarking by Using Genetic Algorithms", IEEE Transactions on Signal Processing, Vol. 53, No. 12, pp. 4707-4719, December, 2005.

[13] H. Daren, L. Jifuen,H. Jiwu, and L. Hongmei, "A DWT-Based Image Watermarking Algorithm", in Proceedings of the IEEE International Conference on Multimedia and Expo, pp. 429-432, 2001.

[14] C. Hsu and J. Wu, "Multi-resolution Watermarking for Digital Images", IEEE Transactions on Circuits and Systems- II, Vol. 45, No. 8, pp. 1097-1101, August 1998.

[15] R. Mehul, "Discrete Wavelet Transform Based Multiple Watermarking Scheme", in Proceedings of the 2003 IEEE TENCON, pp. 935-938, 2003.